2022 IEEE 27th International Conference on Emerging Technologies and Factory Automation (ETFA) | 978-1-6654-9996-5/22/$31.00 ©2022 IEEE | DOI: 10.1109/ETFA52439.2022.9921429

Comparing repetitive control strategies in lift applications

Roberto Fausti
Department of Mechanical and Industrial Engineering
University of Brescia
Brescia, Italy
r.fausti003@studenti.unibs.it

Manuel Beschi
Department of Mechanical and Industrial Engineering
University of Brescia
Brescia, Italy
manuel.beschi@unibs.it

Davide Colombo
Gefran Drives and Motion Srl
Gerenzano, Italy
davide.colombo@gefran.com

Antonio Visioli
Department of Mechanical and Industrial Engineering
University of Brescia
Brescia, Italy
antonio.visioli@unibs.it

***Abstract*—The goal of the control system in lift application in high-speed/high-rise applications is to maximize speed without sacrificing passengers comfort. Lifts are affected by position-based disturbances, which could be compensated by employing a repetitive control strategy. Lifts also have nonlinearities due to the rope mass and stiffness variation with respect to the position. This paper analyzes the performance of LTI position-based repetitive control strategies in lift applications. Simulation with a nonlinear model of the lift shows that repetitive control strategies could improve control performance. In particular, Gaussian Process Repetitive Control is less sensitive to the nonlinearities and provides fewer oscillations.**

***Index Terms*—Repetitive control, lift, disturbance compensation**

I. Introduction

Repetitive Control (RC) is a technique designed to obtain asymptotic perfect tracking on periodic signals. From its first presentation for control of proton synchrotron magnet power supply [1], Repetitive Control has had a wide success both in research and industrial environments because of the repetitive nature of everyday industrial tasks. RC configurations have been implemented in different fields, such as rejection of power supply disturbances [2], control of disk-drive systems [3] and optical disk-drive [4], vibration suppression [5] and robotic manipulators performing repetitive tasks [6], [7].

While multiple configurations have been designed to implement RC techniques, the most common is the digital "plug-in" implementation [8], [9]. This configuration requires to design a low-pass filter, used to reduce the infinite gain of the high-frequency harmonics and thus increasing the robustness, and a stability filter, included to cancel out the phase of the transfer function and stabilize the system.

Several alternative configurations have been presented for different scenarios. A multiple buffer configuration has been proposed to improve the robustness concerning the delay period [10].

One of the main extensions to the method considers the presence of disturbances depending on position instead of time. In fact, several mechanical applications are affected by disturbances related to positional variables like torque ripple, pulleys, bearings, and rail guides [11]–[14]. Initial Repetitive Control strategies focused on time-dependent disturbances providing an effective performance when the system works at constant speeds. However, a position-based repetitive control algorithm is necessary when the constant-speed assumption does not hold. The most frequent approach is the angle-based approach [15], [16], where the buffer obtained by the discretization of the time delay is fed by using the current position instead of the current time. Recent works focused on this problem showing the capability to compensate for the disturbance at the price of increased computational and memory requirements. This aspect makes the implementation challenging in limited-power edge controllers, like the industrial drives. Implementations based on Gaussian Processes have been proposed for the rejection of spatial-domain and multiple domain periodic disturbances [17]–[20].

Various descriptions of possible implementation in nonlinear systems, where the frequency analysis cannot be performed, have been presented in [6], [21]. However, nonlinearities lead to more complex implementations, limiting their usage in industrial motion control. In lift systems, the load mass can change during the task, since the mass of the suspended rope changes depending on the position of the cabin and on the counterweight, as well as the rope elasticity [22], [23]. Load variations can significantly change the resonance/antiresonance frequencies. The variations depend on the state (such as the position of the cabin in the lift example). However, this nonlinearity can be simplified by considering the dependency on the set-point position instead of the actual one. This approximation holds when the dynamics of affected modes vary much quicker than the position variable or when the amplitude of the vibration is negligible with respect to the position variations. Both conditions are verified in the case of high-speed/high-rise lift, thus this class of systems can be described as an LPV system [24].

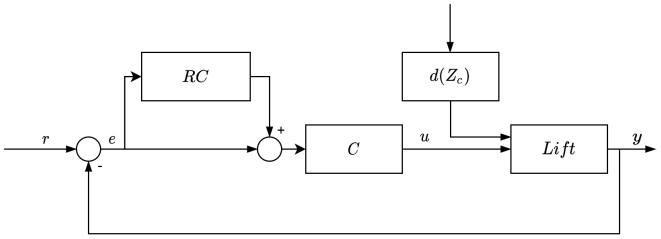

Fig. 1. Angle-based RC scheme.

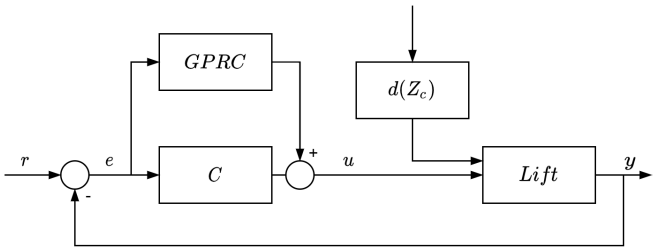

Fig. 2. Gaussian Process RC scheme.

In high-speed/high-rise lifts, the control goal is to maximize the cabin speed while guaranteeing the passengers' comfort, which is strongly related to cabin oscillations. Repetitive disturbances affecting the lift control system are relative to friction between the cabin/counterweight and the rail guide. Finally, cost limitations result in a limited computational power of the control unit.

The contribution aims to analyze the behaviour of linear repetitive control schemes applied to control an LPV system where the disturbances and the parameters depend on the same variable. On the one hand, this requires less computational power with respect to the nonlinear RC methods and less commissioning cost. On the other hand, the model mismatches could affect the achievable performance.

The paper is organized as follows. Section II describes the repetitive control strategies tested in the lift applications. Section III deals with the mathematical model of the lift. Simulations on LTI and LPV systems are carried out in Section IV. Conclusions are drawn in Section V.

II. Compared control strategies

The first considered control strategy is the one presented in [25], shown in Figure 1, which consists of an angle-based method using a memory buffer to store the tracking error. The position is consequently discretized in a set of fixed equidistant positions. The method showed its effectiveness in numerous applications [11], [11], [26]. The method was originally devised for motor control; hence it is designed to work in the range $[0, 2\pi]$; however, it can be easily adapted to a generic periodicity by applying the proper scaling. The method's main advantage is the limited memory usage since it requires storing only a vector.

Then, a new approach which employs a Gaussian process internal model, called Gaussian Process Repetitive Control (GPRC) has been proposed in [18], [20]. This method outperformed previously available schemes when applied to LTI systems, rejecting multi-period and non-periodic disturbances. The method's main drawback is the higher computational burden compared to the angle-based method. The algorithm scheme is shown in Figure 2.

III. Lift model

A lift is a mechanical system where a motor acts on a pulley-rope transmission to move the passenger cabin. A counterweight reduces the maximum motor torque by partially balancing the weight of the cabin and the passengers. The cabin and the counterweight slide on vertical guides; this movement results in horizontal and vertical forces due to friction and misalignment. These forces could generate vibrations and therefore reduce passenger comfort. The horizontal forces are perpendicular to the ropes, resulting in a minimal effect of the motor torque on these vibration modes. Thus, this analysis will neglect them since their compensation does not involve the motor.

As the lift moves, the rope segments connecting the pulley with the cabin and the counterweight change length. The change results in a linear variation of the suspended mass. Moreover, the rope elasticity and damping are a function of the rope length. The rope is a distributed system; however, the lumped system assumption allows a substantial model simplification without losing the main dynamics. The used model considers a rope segment as a variable viscoelastic element connecting the pulley with the centre of the segment, where a variable mass represents the rope's inertial properties; the variable mass is connected with the cabin/counterweight by a second variable viscoelastic element with the same values of the first one.

The resulting model is shown in Figure 3, where the following quantities are considered:

- M_c is the mass of the cabin, which, in case, includes also the presence of passengers;
- M_w is the mass of the counterweight, which is generally equal to the mass of the cabin without passengers;
- M_{rc} is the mass of the rope connected between the cabin and the traction pulley;
- M_{rw} is the mass of the rope connected between the counterweight and the traction pulley;
- M_p is the mass of the pulley used to convert the rotary motion, generated by the electric motor, in a linear motion of the ropes;
- K_c and K_w are the stiffness coefficients, respectively, of the rope's section between the cabin and the traction pulley and of the rope's section which connects the counterweight to the same sheave;
- C_f is the damping coefficient of the ropes;
- R_p is the traction pulley radius;
- J_p is the moment of inertia of the pulley, which is calculated in the center of gravity, comprehensive of the motor and the gearbox contribution.;

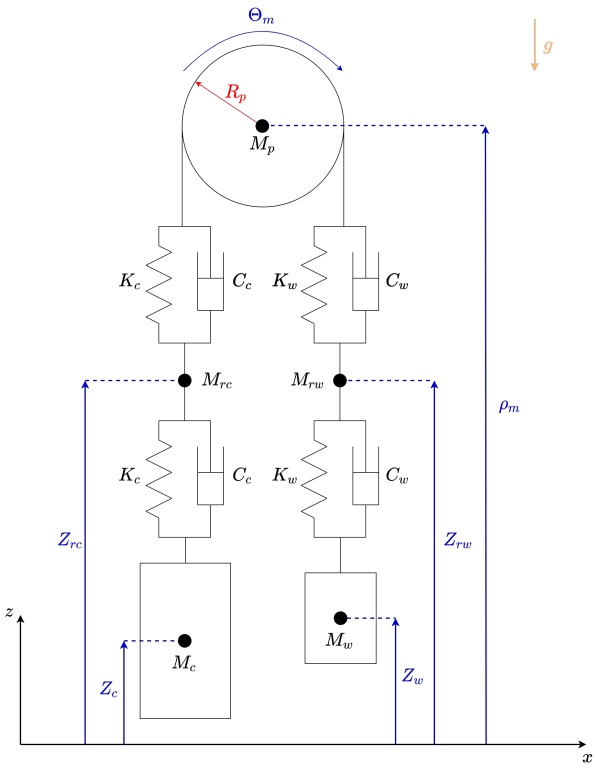

Fig. 3. Schematic scheme of the lift

- h is the viscous friction coefficient of the cabin and the counterweight;
- h_p is the viscous friction coefficient of the pulley;
- ρ_m is the height of the rotation center of the traction pulley, which is calculated from the base of the elevator tower;
- Z_c and Z_w are the vertical position of the cabin and the counterweight, respectively;
- Z_{rc} and Z_{rw} are the vertical position of the lumped mass of the rope segments connecting the pulley with the cabin and the counterweight, respectively;
- Θ_m is the pulley position.

Rope mass is related to the linear density of mass μ of the rope by the formula

$$M_{rc} = \mu \cdot l_c \qquad M_{rw} = \mu \cdot l_w \tag{1}$$

where:

- $l_c = Z_{max} - Z_c$ is the length of the section of rope between the cabin and the traction pulley and Z_{max} is the maximum reachable height;
- $l_w = Z_{max} - Z_w$ is the length of the section of rope between the counterweight and the traction pulley;

The rope stiffness, related to every section of the rope, are evaluated starting from a fixed value of Young's module of the rope:

$$K_c = \frac{2 \cdot E \cdot A}{l_c} \qquad K_w = \frac{2 \cdot E \cdot A}{l_w} \tag{2}$$

where:

- E is Young's module of 1 [m] of rope;
- A is the area of the cross-section of the rope;

Viscous coefficients are not available in the majority of the rope catalogues; therefore, they are assumed to change linearity with the rope length. Their values can be estimated by matching the experimental and the model damping of the vertical vibration modes, that is,

$$C_c = C_f \frac{2l_{c,0}}{l_c}, \quad C_w = C_f \frac{2l_{w,0}}{l_w} \tag{3}$$

where C_c and C_w are the damping factors of the half segments of the cabin and the counterweight, respectively, and $l_{c,0} = l_{w,0}$ are the initial length of the two segments, where the initial condition are assumed with the cabin and the counterweight at the same height.

The manipulated variable is the motor torque u acting on the pulley, while the controlled variable could be the motor position or the motor velocity. In the second case, the positioning is possible by on/off sensors on the building floors. This paper considers the motor position $y = \Theta_m$ as the controlled variable, even if similar results could be obtained in the other scenario. The motor setpoint is indicated with r. The repetitive disturbances $d(Z_c)$ are the vertical forces between the cabin (or the counterweight) and the rail guide.

Applying the conservation of linear and angular momenta, it is possible to write

$$\begin{aligned}
&M_c\ddot{Z}_c = K_c(Z_{rc} - Z_c) + C_c(\dot{Z}_{rc} - \dot{Z}_c) \\
&-M_c g - h\dot{Z}_c + d(Z_c) \\
&M_w\ddot{Z}_w = K_w(Z_{rw} - Z_w) + C_w(\dot{Z}_{rw} - \dot{Z}_w) \\
&-M_w g - h\dot{Z}_w \\
&M_{rc}\ddot{Z}_{rc} + \mu\dot{Z}_{rc} = \\
&-K_c(Z_{rc} - Z_c) - C_c(\dot{Z}_{rc} - \dot{Z}_c) \\
&+K_c(R_p\Theta_m - Z_{rc}) + C_c(R_p\dot{\Theta}_m - \dot{Z}_{rc}) - M_{rc}g \\
&M_{rw}\ddot{Z}_{rw} + \mu\dot{Z}_{rw} = \\
&-K_w(Z_{rw} - Z_w) - C_w(\dot{Z}_{rw} - \dot{Z}_w) \\
&+K_w(-R_p\Theta_m - Z_{rw}) + C_w(-R_p\dot{\Theta}_m - \dot{Z}_{rw}) - M_{rw}g \\
&J_m\ddot{\Theta}_m = \\
&\Big(-K_c(R_p\Theta_m - Z_{rc}) - C_c(R_p\dot{\Theta}_m - \dot{Z}_{rc}) \\
&+K_w(-R_p\Theta_m - Z_{rw}) + C_w(-R_p\dot{\Theta}_m - \dot{Z}_{rw})\Big) R_p \\
&-h_p\dot{\Theta}_m + u
\end{aligned} \tag{4}$$

System (4) results in tenth-order state-space model that can be expressed as in (5).

$$\begin{cases} \dot{x} = A(Z_c)x + Bu + B_d d(Z_c) \\ y = Cx \end{cases} \tag{5}$$

where:

- x is the lift state, containing the position and the velocity of the pulley, of the cabin, of the counterweight, and of the two rope masses;

TABLE I
NUMERICAL VALUE OF THE LIFT MODEL

Parameter	Value
M_c	660 [kg]
M_c	1140 [kg]
M_p	30 [kg]
E	2.1 $\cdot 10^9$ [N/m^2] for each meter
A	100 $\cdot 10^{-6}$ [m^2]
l_c0	39 [m]
l_w0	39 [m]
R_p	0.5 [m]
gear ratio	1/10
C_f	500 [N/(m/s)]
μ	0.8 [kg/m]
J_m	3.75 $\cdot 10^{-4}$ (before gearbox)
h	2 [N/(m/s)]
h_p	15 [Nm/(rad/s)]
Z_{max}	75 [m]

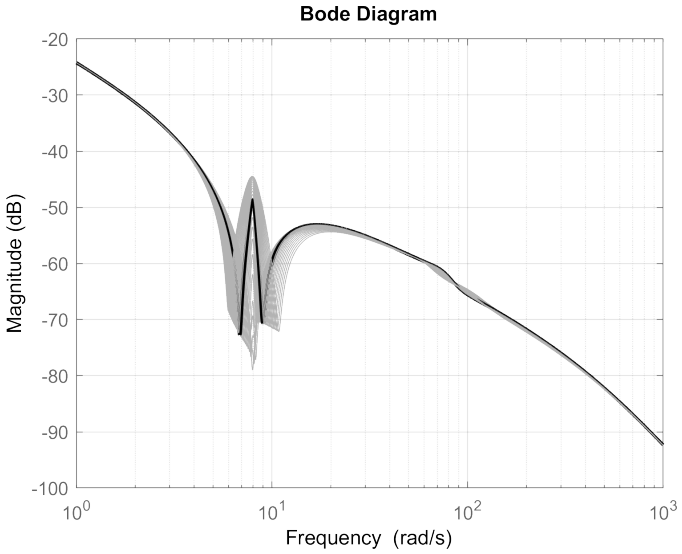

Fig. 4. Bode diagram of the lift model linearized in each floor. Black line represents the middle floor, considered as nominal case.

- u is the motor torque and y is the pulley position;
- the matrix $A(Z_c)$ depends on Z_c, which is a state variable. Thus, this is a nonlinear system in the state-dependant linear form [27]. However, the approximation proposed in Section I holds because the vertical vibrations are orders of magnitude smaller than the cabin movements, allowing replacement in Z_c with its desired value $R_p r$.

IV. SIMULATION ON A LIFT MODEL

Considering the values of the model parameters shown in Table I, representing a lift of 25 floors, the magnitude Bode plot of the linearized plants at each floor is shown in Figure 4. It is worth noticing the shift of the resonance-antiresonance frequency with respect to the nominal case, that is the model linearized at the middle floor.

The disturbance $d(Z_c)$ has two Gaussian-shaped spikes of 200 [N] representing two segments of the rail guide with

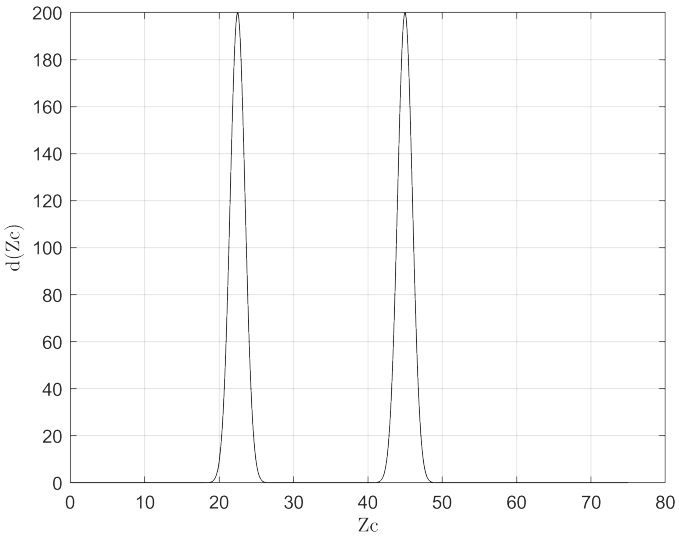

Fig. 5. Shape of the period disturbance $d(Z_c)$.

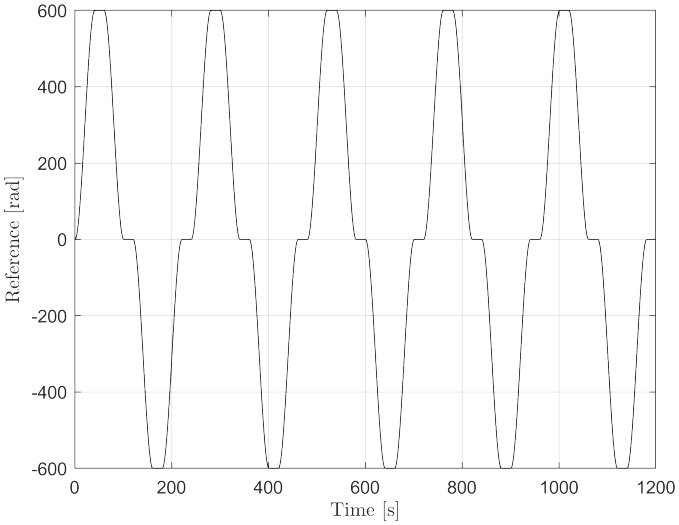

Fig. 6. Shape of the setpoint r. Null value represents the lift at the middle height. The amplitude of the setpoint corresponds to a 10 floors movement of the cabin.

parallel misalignment as shown in Figure 5. The white noise of the position measurement has variance 10^{-6} [m^2].

During the test, the setpoint changes to reach all the lift floors using the jerk-limited trajectory shown in Figure 6.

The controller is a PID algorithm tuned to achieve a bandwidth of 5 rad/s (the first antiresonance frequency is 6.8 rad/s for the nominal model) and a phase margin of 30 degrees. The resulting transfer function is

$$C(s) = 1381 \frac{(s + .667)(s + 2)}{s(s + 60)} \tag{6}$$

The controller works with a sampling period equal to 1 [ms].

The two control strategies described in Section II have been compared with a baseline control algorithm without RC capabilities. Results are shown in Figure 7 and in Figure 8, where a zoom helps to clarify the algorithm performance. The

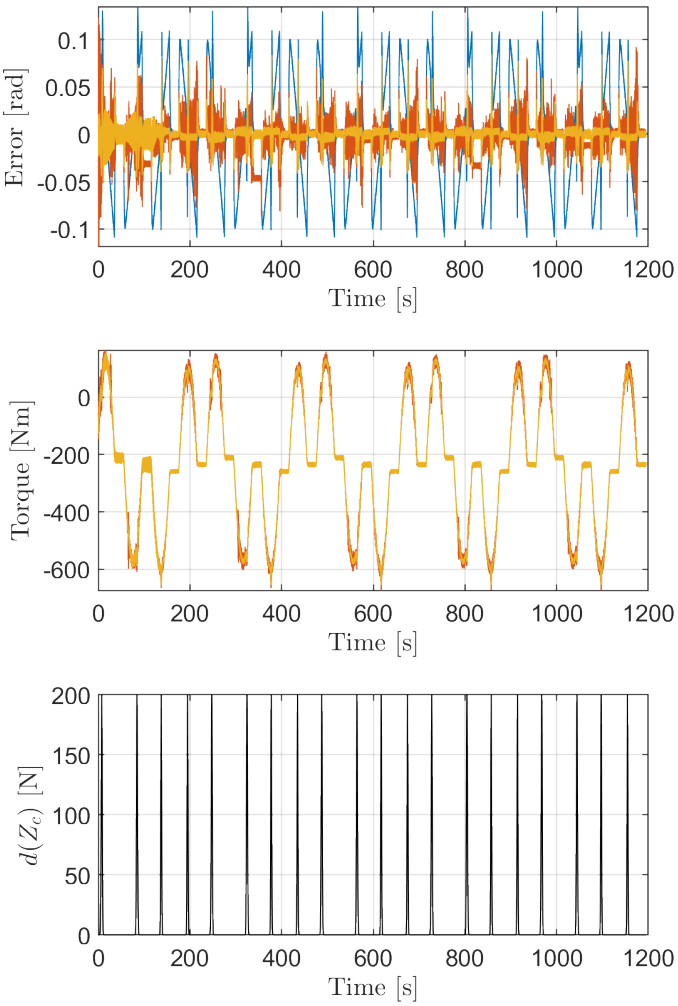

Fig. 7. Simulation results. Trend of the tracking error (top plot): blue line, control system without RC capabilities; red line: control system with angle-based RC algorithm; orange line: control system with Gaussian Process Repetitive Control. Trend of the motor torque (middle plot): blue line, control system without RC capabilities; red line: control system with angle-based RC algorithm; orange line: control system with Gaussian Process Repetitive Control. Trend of the disturbance (bottom plot): black line, force disturbance applied on the cabin, almost identical in the three cases.

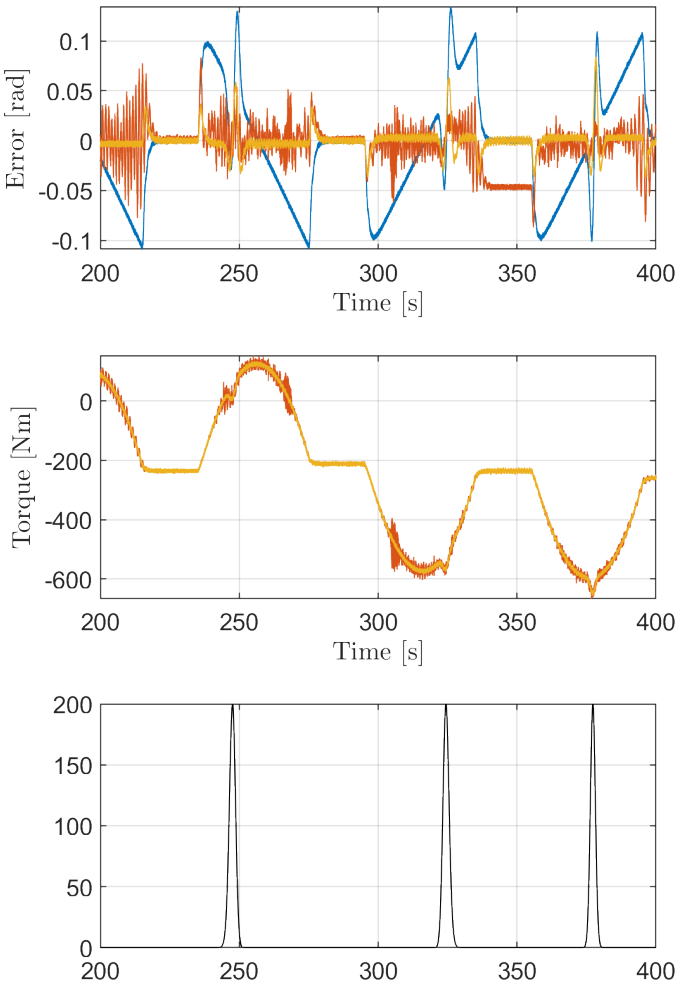

Fig. 8. Zoom of the simulation results in time interval 200 [s] - 400 [s]. Trend of the tracking error (top plot): blue line, control system without RC capabilities; red line: control system with angle-based RC algorithm; orange line: control system with Gaussian Process Repetitive Control. Trend of the motor torque (middle plot): blue line, control system without RC capabilities; red line: control system with angle-based RC algorithm; orange line: control system with Gaussian Process Repetitive Control. Trend of the disturbance (bottom plot): black line, force disturbance applied on the cabin, almost identical in the three cases.

stabilizing filter, required for model inversion, has been chosen to be a low-pass filter with time constant of 0.01 [s].

It is worth noticing that both the RC control strategies outperform the baseline, allowing better setpoint tracking. However, the angle-based algorithm provides more noisy contributions, which result in a high-frequency torque oscillation. This oscillation has a high amplitude when the lift is far from the nominal conditions, where the LTI model does not adequately describe the dynamics.

On the contrary, the Gaussian Process Repetitive Control is much less sensitive to model mismatches, allowing a satisfactory tracking even when the lift is far from the nominal conditions. The oscillations on the motor torque are significantly less than the angle-based approach, which is a clear benefit in achieving higher passenger comfort.

V. Conclusion

This paper shows that repetitive control algorithms reduce the tracking error in a high-speed/high-rise simulated lift. Simulations compared angle-based and Gaussian process repetitive control strategies.

On the one hand, the angle-based algorithm requires fewer computational needs than GPRC, allowing a more straightforward implementation of the motor drives, which have limited computational power due to cost minimization. On the other hand, the angle-based algorithm is more sensitive to the model mismatches between the LTI nominal model and the LPV nature of the lift. For this reason, the angle-based RC provides a higher tracking error and causes oscillation in the motor torque.

Finally, it is worth mentioning that in lift applications,

the disturbance, the target variable, and the sensor are not collocated in the same physical place. The disturbance source is due to the rail guides of the cabin/counterweight, the sensor is typically an encoder mounted on the motor shaft, and the target variable is the position of the cabin. In this class of applications, nullifying the motor-velocity error could lead to more oscillations and discomfort (namely, higher accelerations) of the target variable. For this reason, the angled-based RC algorithm needs further investigations to enable its implementation in the considered scenario. In future works, the knowledge of disturbance estimation could mitigate these aspects by changing the system's behaviour, for example, by reducing speed or changing motor law.

ACKNOWLEDGMENT

This research has received funding from the ECSEL Joint Undertaking under grant agreement 101007311 (IMOCO4.E). The Joint Undertaking receives support from the European Union's Horizon 2020 research and innovation program.

REFERENCES

[1] T. Inoue, M. Nakano, T. Kubo, S. Matsumoto, and H. Baba, "High accuracy control of a proton synchrotron magnet power supply," *IFAC Proceedings Volumes*, vol. 14, pp. 3137–3142, 8 1981.

[2] M. Nakano and S. Hara, "Microprocessor-based repetitive control," *Microprocessor-Based Control Systems*, pp. 279–296, 1986.

[3] K. K. Chew and M. Tomizuka, "Digital control of repetitive errors in disk drive systems," *IEEE Control Systems Magazine*, vol. 10, pp. 16–20, 1990.

[4] J. H. Moon, M. N. Lee, and M. J. Chung, "Repetitive control for the track-following servo system of an optical disk drive," *IEEE Transactions on Control Systems Technology*, vol. 6, pp. 663–670, 1998.

[5] S. Hattori, M. Ishida, and T. Hori, "Vibration suppression control method for pmsm utilizing repetitive control with auto-tuning function and fourier transform," *IECON Proceedings (Industrial Electronics Conference)*, vol. 1, pp. 1673–1679, 2001.

[6] T. Omata, S. Hara, and M. Nakano, "Nonlinear repetitive control with application to trajectory control of manipulators," *Journal of Robotic Systems*, vol. 4, pp. 631–652, 10 1987.

[7] L. Biagiotti, L. Moriello, and C. Melchiorri, "A repetitive control scheme for industrial robots based on b-spline trajectories," *IEEE International Conference on Intelligent Robots and Systems*, vol. 2015-December, pp. 5417–5422, 12 2015.

[8] G. A. Ramos, R. Costa-Castelló, and J. M. Olm, *Digital Repetitive Control under Varying Frequency Conditions*. Springer Berlin Heidelberg, 2013, vol. 446.

[9] M. Tomizuka, T. C. Tsao, and K. K. Chew, "Discrete-time domain analysis and synthesis of repetitive controllers." *Proceedings of the American Control Conference*, vol. 88 pt 1-3, pp. 860–866, 1988.

[10] M. Steinbuch, S. Weiland, and T. Singh, "Design of noise and period-time robust high-order repetitive control, with application to optical storage," *Automatica*, vol. 43, pp. 2086–2095, 12 2007.

[11] M. Tang, P. Zanchetta, A. Gaeta, and A. Formentini, "A variable frequency angle-based repetitive control for torque ripple reduction in pmsms," vol. 2016. Institution of Engineering and Technology, 2016, pp. 6 .–6 . [Online]. Available: https://digital-library.theiet.org/content/conferences/10.1049/cp.2016.0325

[12] M. Tang, A. Formentini, S. A. Odhano, and P. Zanchetta, "Torque ripple reduction of pmsms using a novel angle-based repetitive observer," *IEEE Transactions on Industrial Electronics*, vol. 67, pp. 2689–2699, 4 2020.

[13] J. Liu, H. Li, and Y. Deng, "Torque ripple minimization of pmsm based on robust ilc via adaptive sliding mode control," *IEEE Transactions on Power Electronics*, vol. 33, pp. 3655–3671, 4 2018.

[14] T. Oomen, "Advanced motion control for precision mechatronics: control, identification, and learning of complex systems," *IEEJ Journal of Industry Applications*, vol. 7, pp. 127–140, 1 2018. [Online]. Available: https://research.tue.nl/en/publications/advanced-motion-control-for-precision-mechatronics-control-identi

[15] C. J. Chien and K. Y. Ma, "Feedback control based sampled-data ilc for repetitive position tracking control of dc motors," *2013 CACS International Automatic Control Conference, CACS 2013 - Conference Digest*, pp. 377–382, 2013.

[16] M. Tang, A. Gaeta, A. Formentini, K. Ohyama, P. Zanchetta, and G. Asher, "Enhanced dbcc for high-speed permanent magnet synchronous motor drives," *IET Power Electronics*, vol. 9, pp. 2880–2890, 12 2016. [Online]. Available: https://nottingham-repository.worktribe.com/output/836547/enhanced-dbcc-for-high-speed-permanent-magnet-synchronous-motor-drives https://nottingham-repository.worktribe.com/output/836547/enhanced-dbcc-for-high-speed-permanent-magnet-synchronous-motor-drives.abstract

[17] M. Goubej, S. Meeusen, N. Mooren, and T. Oomen, "Iterative learning control in high-performance motion systems: From theory to implementation," *IEEE International Conference on Emerging Technologies and Factory Automation, ETFA*, vol. 2019-September, pp. 851–856, 9 2019.

[18] N. Mooren, G. Witvoet, I. Acan, J. Kooijman, and T. Oomen, "Suppressing position-dependent disturbances in repetitive control: With application to a substrate carrier system." IEEE, 9 2020, pp. 331–336. [Online]. Available: https://ieeexplore.ieee.org/document/9244347/

[19] N. Mooren, G. Witvoet, and T. Oomen, "Gaussian process repetitive control for suppressing spatial disturbances," *IFAC-PapersOnLine*, vol. 53, pp. 1487–1492, 1 2020. [Online]. Available: https://linkinghub.elsevier.com/retrieve/pii/S2405896320325659

[20] ——, "Gaussian process repetitive control: Beyond periodic internal models through kernels," *Automatica*, vol. 140, p. 110273, 6 2022.

[21] F. Califano, M. Bin, A. MacChelli, and C. Melchiorri, "Stability analysis of nonlinear repetitive control schemes," *IEEE Control Systems Letters*, vol. 2, pp. 773–778, 10 2018.

[22] D. Santo, J. Balthazar, A. Tusset, V. Piccirilo, R. Brasil, and M. Silveira, "On nonlinear horizontal dynamics and vibrations control for high-speed elevators," *Journal of Vibration and Control*, vol. 24, 08 2016.

[23] R. Roberts, "Control of high-rise/high-speed elevators," in *Proceedings of the 1998 American Control Conference. ACC (IEEE Cat. No.98CH36207)*, vol. 6, 1998, pp. 3440–3444 vol.6.

[24] F. Amato, "Robust control of linear systems subject to uncertain time-varying parameters," *Lecture Notes in Control and Information Sciences*, vol. 325, pp. 1–194, 2006.

[25] S. K. Sahoo, S. K. Panda, and J. X. Xu, "Application of spatial iterative learning control for direct torque control of switched reluctance motor drive." IEEE, 6 2007, pp. 1–7. [Online]. Available: http://ieeexplore.ieee.org/document/4275420/

[26] Y. Yuan, F. Auger, L. Loron, S. Moisy, and M. Hubert, "Torque ripple reduction in permanent magnet synchronous machines using angle-based iterative learning control," *IECON Proceedings (Industrial Electronics Conference)*, pp. 2518–2523, 2012.

[27] S. Saat, S. K. Nguang, and A. Nasiri, "Analysis and synthesis of polynomial discrete-time systems: An sos approach," *Analysis and Synthesis of Polynomial Discrete-Time Systems: An SOS Approach*, pp. 1–187, 7 2017.